Miner Deposita (2006) 41: 188–200
DOI 10.1007/s00126-006-0058-6

ARTICLE

Lianchang Zhang · Wenjiao Xiao · Kezhang Qin · Qi Zhang

The adakite connection of the Tuwu–Yandong copper porphyry belt, eastern Tianshan, NW China: trace element and Sr-Nd-Pb isotope geochemistry

Received: 7 May 2005 / Accepted: 4 March 2006 / Published online: 31 March 2006

Abstract The Tuwu–Yandong porphyry copper belt lies in the eastern Tianshan mountains, eastern section of the Central Asian orogenic belt. The copper mineralization is mainly hosted in plagiogranite porphyries intruded into early Carboniferous volcanic rocks of the Paleozoic Dananhu island arc between the Tarim and Siberian plates. The plagiogranite porphyries have contents of 65–73 wt% SiO_2, 14–17 wt% Al_2O_3, 0.9–2.2 wt% MgO, 3–16 ppm Y, 0.4–1.40 ppm Yb, 347–920 ppm Sr, and positive Eu anomalies. The rocks also exhibit positive $\varepsilon_{Nd(t)}$ values (+5.0 to +9.4) and low initial $^{87}Sr/^{86}Sr$ values (0.70316–0.70378). Such features are similar to those of adakites derived from partial melting of a subduction-related oceanic slab. The mineralization age is early Carboniferous (350–320 Ma), which is close to that of the porphyries. The close relationship between the Cu mineralization and the porphyry is also indicated by their similar Sr-Nd-Pb isotopic compositions. We suggest that the copper porphyry (magma) system in the Dananhu island arc was formed by direct melting of an obliquely subducting early Carboniferous oceanic slab.

Keywords Adakite · Porphyry copper deposit · Island arc · Late Paleozoic · East Tianshan

Introduction

Over a decade ago Defant and Drummond (1990) and Drummond and Defant (1990) proposed that adakites are products of the melting of young subducted oceanic crust and that the Archean continental tonalite-trondhjemite-granodiorite crust was generated primarily by slab melting. Gold and copper mineralization is commonly associated with the adakite volcanic series in the Pacific Rim (Thiéblemont et al. 1997; Sajona and Maury 1998; Oyarzún et al. 2001; Zhang et al. 2002; Defant et al. 2002; Mungall 2002). Adakitic rocks in China occur in mid-Miocene continental collision zones in southern Tibet (Chung et al. 2003) and in late Paleozoic island arcs in northern Xinjiang (Xiong et al. 2001; Xu et al. 2001). Some ore-bearing porphyries in the Gangdese belt of Tibet exhibit the characteristics of adakites (Qu et al. 2004; Hou et al. 2004).

The Tuwu and Yandong superlarge porphyry Cu deposits were discovered in the eastern Tianshan, NW China in the late 1990s (Wang et al. 2001). These porphyry Cu deposits are located in the southern section of the Dananhu island arc about 80 km southwest of Hami City, eastern Xinjiang (Fig. 1). These and other porphyry occurrences, such as Chihu, Linglong, and Sanchakou, form the Tuwu–Yandong copper ore belt. Initial reports by the No. 1 Geological Team indicate that the Tuwu and Yandong porphyry deposits contain about 4.7 million tons of copper at an average grade of 0.67% Cu. In addition, the deposits are estimated to contain 18 ton of Au at an average grade of 0.2 g/ton and significant amounts of Ag and Mo (Wang et al. 2001; Liu et al. 2003). The ore potential of the eastern Tianshan is highlighted by the recent discovery of the world-class Oyu Tolgoi Cu-Au-Mo porphyry district in the Gobi desert of southern Mongolia (Perello et al. 2001), which has a similar geological setting.

Since the discovery of the Tuwu and Yandong deposits, extensive investigations were carried out on their ore geology (Wang et al. 2001; Rui et al. 2002; Liu et al. 2003; Han et al. 2003) and isotope geochronology (Rui et al. 2002; Liu et al. 2003). However, some scientific problems, such as geological setting, geochemical features, and ore-forming mechanism of the porphyries, remain poorly understood. Based on our field investigations and geochemical studies, we suggest that the late Paleozoic ore-bearing porphyries in the Tuwu–Yandong area have

Editorial handling: B. Lehmann

L. Zhang (✉) · W. Xiao · K. Qin · Q. Zhang
Key Laboratory of Mineral Resources,
Institute of Geology and Geophysics,
Chinese Academy of Sciences,
P.O. Box 9825, Beijing 100029, China
e-mail: lczhang@mail.igcas.ac.cn
Tel.: +86-10-62008126
Fax: +86-10-62010846

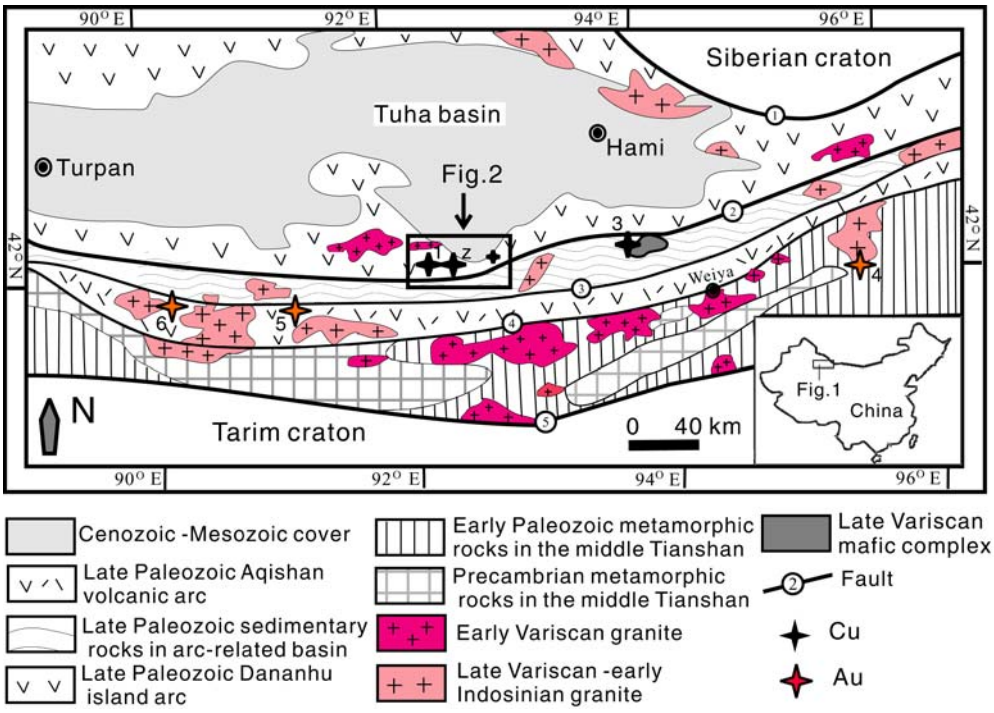

Fig. 1 Simplified geological map of the eastern Tianshan, NW China (after Zhang et al. 2005). *Numbers1–6* show location of ore deposits: *1* Tuwu Cu (Mo) deposit, *2* Yandong Cu (Mo) deposit, *3* Huangshan Cu-Ni deposit, *4* Jinwozi Au deposit, *5* Kanggur Au deposit, and *6* Shiyingtan Au deposit. *1* Kalamaili fault, *2* Kanggurtag fault, *3* Kushui fault, *4* Weiya fault, and *5* Kumishi fault

adakitic characteristics and are comparable to ore-bearing porphyries in the Pacific Rim and southern Tibet. This paper reports major element, trace element, and Sr-Nd-Pb isotope data of the adakites in the late Paleozoic Dananhu island arc in the eastern Tianshan. The mineralization and geodynamic implications of the adakitic rocks are also addressed.

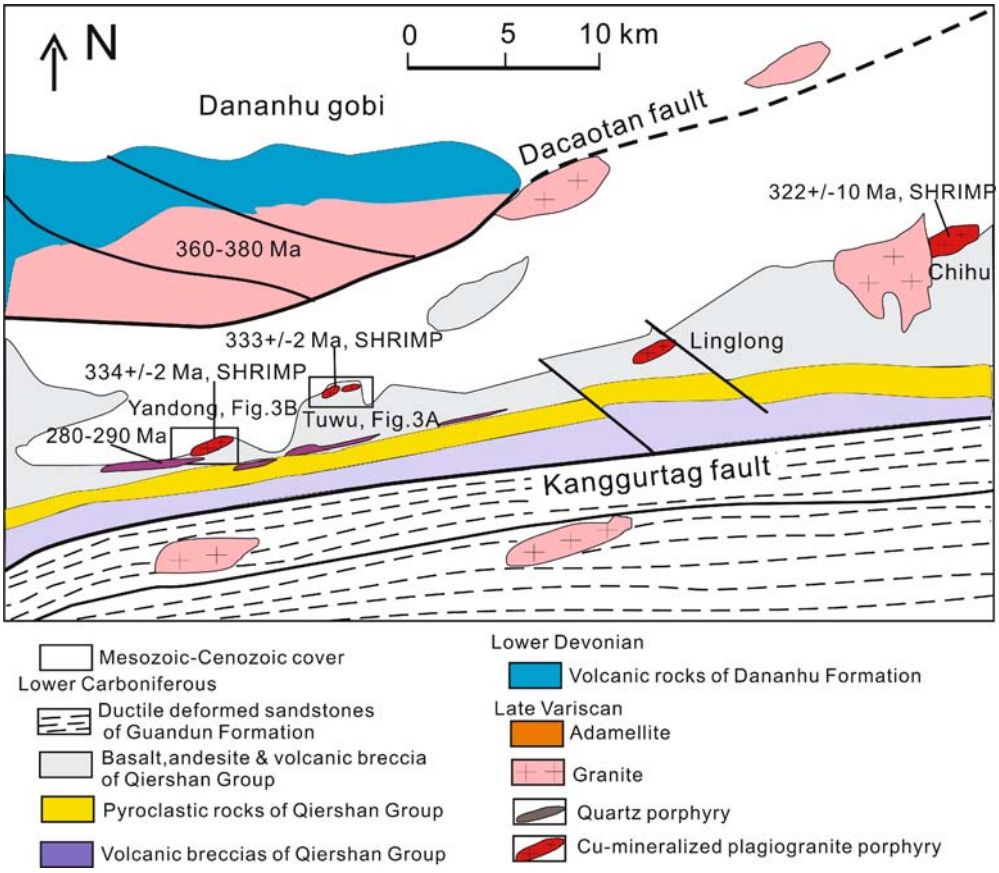

Fig. 2 Regional geological map of the Tuwu–Yandong porphyry copper belt in the eastern Tianshan (modified from Liu et al. 2003)

Geological setting and deposit geology

Geological setting

The eastern Tianshan mountains are part of the central Asian Paleozoic accretionary and collisional orogenic belt between the Siberian and Tarim plates (Windley et al. 1990; Allen et al. 1992; He et al. 1994; Gu et al. 1999, 2001; Qin et al. 2002, 2003; Xiao et al. 2004). The main structures of the orogen are characterized by a series of approximately east-west-trending faults, including the Kalamaili fault/suture, Kanggurtag fault/suture, and Kushui, Weiya, and Kumishi faults (Fig. 1). Of these, the Kanggurtag fault is the most important because it was the locus of intense magmatism and associated mineralization (Ma et al. 1997; Zhang et al. 2004a,b, 2005). The Paleozoic Dananhu island arc, which is mainly composed of Devonian to Carboniferous volcanic-intrusive rocks with genetically affiliated porphyry copper deposits (e.g., Tuwu, Yandong, Linglong and Chihu) occurs to the north of the Kanggurtag fault (Figs. 1 and 2). The late Paleozoic Kanggurtag–Huangshan arc-related basin consisting of Carboniferous sedimentary rocks is located between the Kanggurtag and Kushui faults (Zhang et al. 2003).

Intrusions in the eastern Tianshan are dominated by Variscan (380–270 Ma) granite, plagiogranite porphyry, tonalite, quartz porphyry, dacitic porphyry, and mafic–ultramafic bodies.

The development of most metal deposits in eastern Tianshan was closely related to the accretion and collision between the Tarim and Siberian plates (He et al. 1994; Qin et al. 2003; Xiao et al. 2004). The Dananhu magmatic arc and associated porphyry copper deposits were formed during the accretion of the Devonian to early Carboniferous island arc. In late Carboniferous time, the Tianshan Ocean was closed and continent–continent collision led to the formation of the eastern Tianshan orogen and orogenic Au deposits (Zhang et al. 2003). The collision was

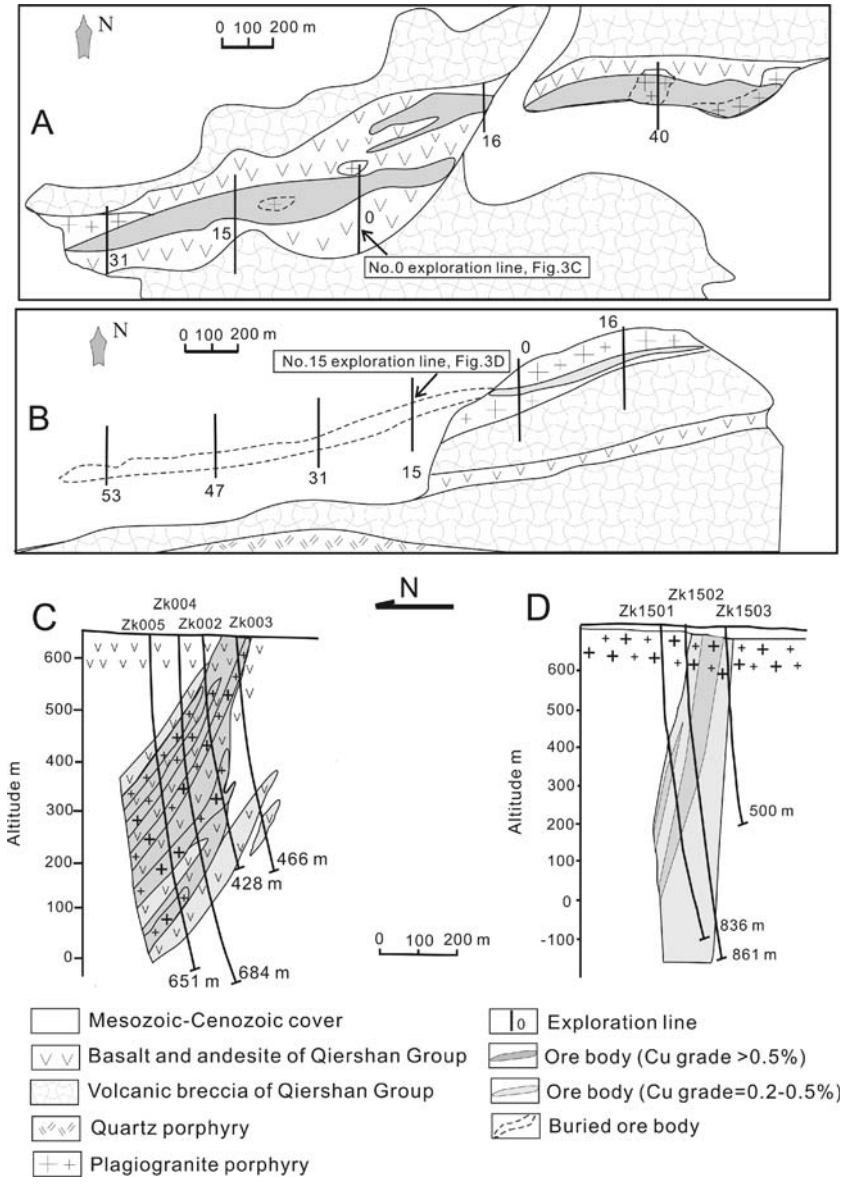

Fig. 3 Geological map of the Tuwu (**a**) and Yandong (**b**) porphyry copper deposit and geological exploration section of the Tuwu (**c**) and Yandong (**d**) ore deposit (modified from Liu et al. 2003)

followed by an extensional event in the Permian that resulted in the emplacement of ultramafic–mafic complexes associated with major magmatic copper–nickel deposits along the Kanggurtag fault (Zhang et al. 2004a, 2005).

Ore-bearing porphyries and mineralization

The Tuwu and Yandong porphyry copper deposits are located about 2–5 km north of the Kanggurtag fault and are mainly hosted in plagiogranite porphyries that were intruded in early Carboniferous intermediate to mafic volcanic rocks of the Qiershan Group (Liu et al. 2003). Devonian volcanic rocks of the Dananhu Formation and an adamellite body (360–380 Ma, Jiang et al., unpublished data) are exposed north of the Dacaotan fault (Fig. 2). An EW-trending quartz porphyry vein is located in the southern ore area. Based on geology and isotopic ages (280–290 Ma, Li et al. 2005 unpublished data), it is indicated that the quartz porphyry was intruded post ore. The deposits are 8 km apart and are poorly exposed. The Linglong and Chihu deposits are located 15 km and 30 km to the east of Tuwu, respectively (Fig. 2), and have similar features to those of the Tuwu and Yandong deposits, but they were not studied in detail.

The ore-bearing intrusions at Tuwu and Yandong are plagiogranite porphyries (Liu et al. 2003). In the Tuwu area, there are 23 plagiogranite-porphyry intrusions; the largest is ~0.03 km^2 in area and all other bodies are <0.01 km^2 with the smallest being <100 m^2. They are mostly irregular in shape on the surface (Fig. 3a) and occur as apophyses if viewed on geological exploration sections (Fig. 3c). In the Yandong area, some larger porphyry bodies are exposed (Fig. 3b,d). These rocks are massive and porphyritic in texture. Phenocrysts of plagioclase and quartz occur in a matrix consisting of quartz, plagioclase, and hornblende. Plagioclase phenocrysts (Fig. 4a,b) fall into two grain-size ranges: The larger have a grain size of 2–4 mm and account for 5vol.% of the rock and the smaller are 0.2–0.5 mm in grain size and generally make up 10vol.% of the rocks. Microcrystalline plagioclase and quartz occupy 30vol.% of the rocks. Hydrothermal alteration is represented by strong silicification, sericitization, and biotitization (Fig. 4c,d).

The mineralized bodies have elongate shape with their long axes parallel to their porphyry hosts. The Tuwu deposit comprises two larger orebodies. Orebody I is 1,400-m-long, 10- to 130-m-thick, and dips toward 180° at angles of 65–80°. Orebody II extends for 1,300 m and is 10 to 84 m in width. In the dip direction, the orebodies extend over 600 m below the surface (Fig. 3a,c). The main orebody in the Yandong deposit extends for over 1,000 m

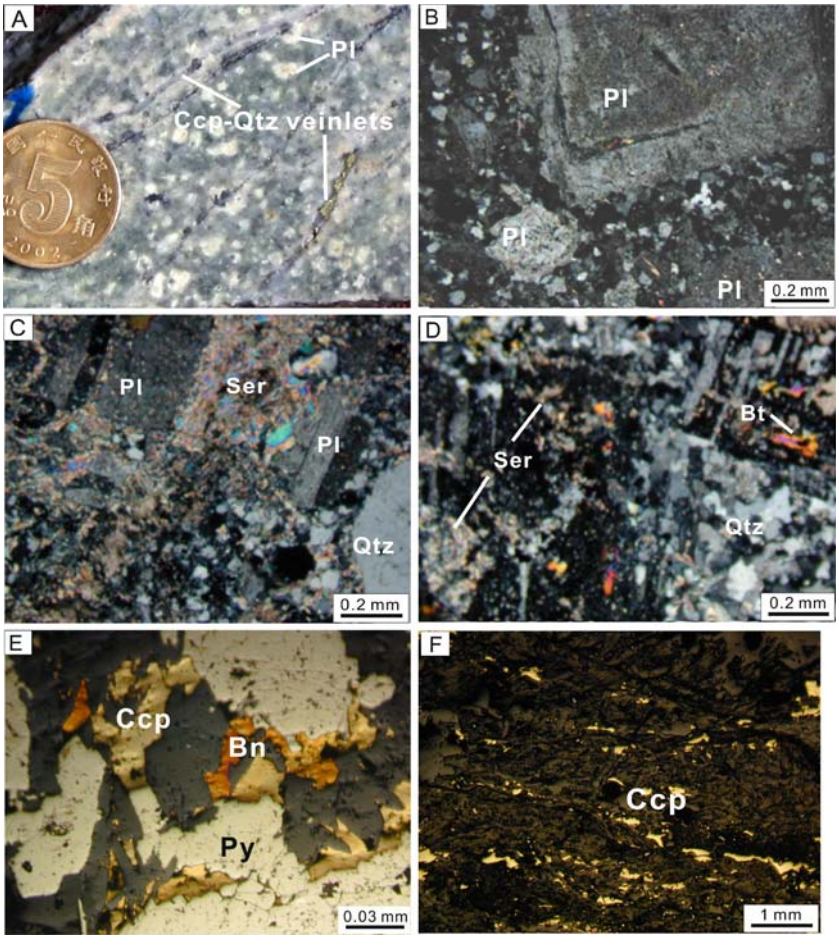

Fig. 4 Photomicrographs of porphyries and ores. **a** Massive plagiogranite porphyry and chalcopyrite (*Ccp*)-quartz (*Qtz*) veinlets. **b** Plagioclase phenocrysts and matrix consisting of quartz (*Qtz*) and plagioclase (*Pl*). **c** Plagioclase phenocrysts (*Pl*) with sericitization. **d** Alteration features of plagiogranite porphyry; the alteration minerals include quartz (*Qtz*), sericite (*Ser*), and biotite (*Bt*). **e** Polished section showing the sulfide assemblage consisting of chalcopyrite (*Ccp*), pyrite (*Py*), and bornite *(Bn*). **f** Polished section showing veinlet-disseminated chalcopyrite mineralization in the plagiogranite porphyry

in length and is 10- to 382-m-wide (Fig. 3b). Ore minerals in the Tuwu and Yandong deposits are dominated by chalcopyrite and pyrite with minor bornite (Fig. 4e), chalcocite, magnetite, sphalerite, and hessite. Gangue minerals are mainly composed of quartz and oligoclase with minor sericite, chlorite, biotite, amphibole, and epidote. Ore minerals occur as disseminations and veinlets (Fig. 4a,f). Biotite is closely associated with the main ore zones but K-feldspar is absent (Rui et al. 2002). Wallrock alteration closest to the ore zones is dominated by silicification (20 to 125 m in width) that gives way outward to silicification–sericitization (10 to 65 m in width), then to sericitization–kaolinitization (10 to 70 m in width), and finally to an outer epidote-rich halo (20 to 85 m in width).

Mineralization took place in four stages. Stage 1 is characterized by disseminations with a chalcopyrite + bornite + pyrite assemblage; Stage 2 is represented by veins containing quartz + pyrite + chalcopyrite; Stage 3 is featured by a quartz + molybdenite assemblage both in veins and as disseminations; and Stage 4 is characterized by an assemblage of carbonates (calcite) + laumontite + minor sulfides.

Ages of ores and their host porphyries

The volcanic rocks of the Qiershan Group in the Dananhu arc are commonly suggested to be Devonian to early Carboniferous, although there are no robust isotopic ages. However, the ages of the ores and their porphyries at Tuwu and Yandong are well determined (Table 1). Quartz and sericite in ores yielded an ^{40}Ar-^{39}Ar age of 347.3±2.1 Ma and a K-Ar age of 341±4.9 Ma (Qin et al. 2002). Re-Os dating of molybdenites of the early and late mineralization stages yielded two ages of 343±26 Ma (Zhang et al. 2004b) and 322.7±2.3 Ma (Rui et al. 2002). The plagiogranite porphyries have single-grain zircon U-Pb ages of 356–361 Ma (Qin 2002; Rui et al. 2002) and SHRIMP zircon U-Pb ages of 333–334 Ma (Liu et al. 2003). These data indicate that the porphyries range in age from 361 to 333 Ma and the ores between 347 and 323 Ma. The above results exhibit two groups of ages: 356–361 Ma and 322–334 Ma for the ore-bearing porphyries and 341–347 Ma and 322 Ma for the ores. Further work is required to clarify whether the age differences were induced by different dating methods or really represent two mineralization events. However, the ores and their host porphyries are early Carboniferous and hence, comparable to the Oyu Tolgoi porphyry copper deposit in southern Mongolia that has a Re-Os molybdenite age of 372±1.2 Ma for the ore (Stein 2003, unpublished data), U-Pb zircon SHRIMP ages of 370–378 Ma for the ore-hosting porphyries (Brimhall 2003, unpublished data), and 335±3 Ma for rhyolite (Wainwright et al. 2004, unpublished data).

Geochemistry and Sr-Nd-Pb isotopic composition

Samples of the ore-hosting porphyries were collected from the Tuwu and Yandong ore districts. Owing to relatively extensive alteration in these districts, the porphyries were more or less affected by biotitization, silicification, sericitization, and propylitization. The least altered samples were chosen for major element, trace element, and Sr-Nd-Pb isotope analyses. In addition, samples of postore porphyries (quartz porphyries) and arc volcanic rocks (basalts and andesites) were collected and analyzed. Results are listed in Tables 2, 3, and 4. Analyses were performed at the Institute of Geology and Geophysics, Chinese Academy of Sciences. Major elements were determined on a PHILIPS PW-1400 X-ray fluorescence spectrometer with precision better than 1%, trace elements on a Finnigan ELEMENT-2 mass spectrometer with a detection limit of 0.01 ppm, and Sr-Nd-Pb isotopes on a MAT262 mass spectrometer. Details of the chemical procedures were described by Chen et al. (2002).

Major and trace elements

The results in Table 2 show that SiO_2, Al_2O_3 and MgO contents of the ore-bearing plagiogranite porphyries range from 65–73, 14–17, and 0.9–2wt%, respectively; Na_2O and K_2O contents from 3–6 and 1–2wt%, respectively; and Na_2O/K_2O ratios from 1.3–4.6. The magnesian index

Table 1 Age data of ores and ore-bearing porphyries in the Tuwu–Yandong copper belt

Geological position	Sample material	Dating method	Age (Ma)	Reference
Postores	Quartz porphyry	SHRIMP U-Pb	280–290[a]	Li et al. 2005
Ore	Molybdenite	Re-Os isochron	322.7±2.3	Rui et al. 2002
	Molybdenite	Re-Os isochron	343±26	Zhang et al. 2004b
	Sericite	K-Ar	341.2±4.9	Qin et al. 2002
	Quartz	Ar-Ar	347.3±2.1	Qin et al. 2002
Host rocks	Plagiogranite porphyry	SHRIMP U-Pb	333±2	Liu et al. 2003
		SHRIMP U-Pb	334±2	Liu et al. 2003
		SHRIMP U-Pb	322±10 (Chihu)[a]	Li et al. 2005
		Single zircon U-Pb	361±8	Rui et al. 2002
		Single zircon U-Pb	356±8	Qin et al. 2002

[a]Unpublished data

Table 2 Major (wt%) and trace element (ppm) abundance of representative rocks in the Tuwu–Yandong ore belt

Sample	PG-P YD203	PG-P YD-34	PG-P TW208	PG-P TW203	PG-P TW306	PG-P TW18	PG-P RY-1[a]	PG-P RY-2[a]	PG-P TW-33	PG-P TW-35	B TW206-2	B TW202-1	A YD305	A TW201	Q-P YD205-1	Q-P YD205-2
SiO_2	70.12	68.76	68.21	70.32	70.62	64.92	72.28	67.50	69.76	73.05	50.02	52.24	62.53	56.34	76.64	78.83
TiO_2	0.27	0.38	0.37	0.26	0.29	1.23	0.21	0.24	0.40	0.34	1.03	1.07	1.06	1.66	0.10	0.18
Al_2O_3	15.59	15.89	17.08	16.15	17.03	16.42	14.52	14.8	15.89	14.24	18.63	17.05	17.89	17.10	12.70	12.06
Fe_2O_3	1.31	2.34	1.60	1.40	0.78	2.08	1.34	1.87	1.10	1.70	2.65	3.27	3.37	3.71	1.28	1.25
FeO	0.87	1.30	1.31	0.76	0.86	2.40	1.78	1.72	1.05	1.07	5.73	4.42	3.48	5.90	0.74	0.56
MnO	0.03	0.02	0.03	0.02	0.02	0.14	0.11	0.08	0.03	0.02	0.26	0.11	0.04	0.15	0.06	0.02
MgO	0.93	1.24	1.35	0.92	0.97	2.16	1.33	1.25	1.28	1.17	7.51	5.35	3.73	3.96	0.75	0.48
CaO	2.05	1.01	1.56	1.10	1.11	3.49	1.45	3.40	1.22	0.30	6.45	8.23	1.63	4.48	0.54	0.11
Na_2O	5.60	2.98	4.89	5.24	4.73	3.35	3.42	4.21	4.93	3.45	2.78	2.99	3.28	4.06	4.83	2.34
K_2O	1.22	2.35	2.00	2.05	2.14	1.78	1.91	1.97	1.56	1.13	1.21	1.44	1.24	0.86	1.59	2.09
P_2O_5	0.08	0.21	0.12	0.08	0.06	0.55	0.11	0.12	0.30	0.37	0.17	0.26	0.11	0.21	0.02	0.01
LOI	1.78	2.93	1.52	1.68	1.41	0.91	1.00	2.06	2.30	2.50	3.33	3.00	1.68	1.39	1.29	1.60
Total	99.85	99.41	100.04	99.98	100.02	99.43	99.46	99.22	99.82	99.34	99.77	99.45	100.04	99.82	99.54	99.93
$Mg^{\#}$	45	42	46	44	46	41	44	40	48	46	50	48	45	43	31	38
Ba	786	605	1,483	850	586	554			458	272	2,353	2,262	1,228	1,628	277	142
Cs	1.90	1.20	3.57	2.43	1.21	1.18			0.46	1.01	1.03	1.08	4.88	1.57	1.02	0.90
Rb	17.0	9.79	46.6	35.0	21.8	18.5			11.5	23.0	11.4	26.3	89.7	9.34	51.6	56.4
Sr	738	347	619	347	714	920			421	397	664	828	294	800	65.4	35.4
Y	8.94	13.3	6.17	4.42	5.23	16.0	3.39	5.94	6.30	6.03	19.4	19.1	11.6	25.3	39.1	43.2
Cr	45.9	184	15.7	15.7	16.6	111			17.9	11.9	134	118	94.4	28.0	16.3	14.4
Ni	34.2	109	2.70	2.63	6.80	79.9			12.8	8.14	105	66.5	63.8	10.1	3.15	3.14
Nb	1.44	2.74	3.15	2.72	2.21	8.39			2.18	3.05	4.13	6.13	4.83	5.09	17.1	16.4
Zr	37.4	73.8	41.9	15.6	37.0	146			86.7	74.3	103	162	140	184	231	227
Hf	1.06	1.89	1.23	0.59	1.09	3.53			2.29	2.00	2.81	4.19	3.46	5.20	7.14	7.03
Ta	0.16	0.21	0.32	0.44	0.12	0.56			0.21	0.28	0.75	2.52	0.80	0.55	1.57	1.53
La	6.28	6.73	11.4	7.38	7.71	16.5	5.17	8.79	7.33	9.94	14.3	16.8	9.62	12.5	40.6	41.7
Ce	14.4	16.37	23.5	15.1	15.5	36.1	10.5	16.7	15.2	20.1	28.9	40.2	23.1	30.2	90.1	95.5
Pr	1.93	2.25	2.78	1.79	1.83	4.44	1.04	1.97	1.77	2.33	4.07	5.27	3.07	4.21	11.0	11.4
Nd	8.58	10.5	11.0	6.83	7.19	18.8	4.19	9.21	6.86	8.69	18.1	22.8	13.2	18.8	40.5	41.5
Sm	2.04	2.60	1.93	1.21	1.27	3.86	0.85	1.34	1.39	1.45	4.08	4.68	2.76	4.57	7.91	8.13
Eu	0.78	1.01	0.81	0.59	0.60	1.28	0.38	0.62	0.54	0.42	1.75	1.79	0.87	1.71	0.56	0.60
Gd	2.07	2.88	1.60	1.05	1.19	3.80	0.86	1.54	1.25	1.10	4.09	4.42	2.58	4.69	6.99	7.62
Tb	0.29	0.41	0.20	0.13	0.16	0.50	0.13	0.25	0.19	0.17	0.61	0.64	0.34	0.75	1.14	1.21
Dy	1.70	2.38	1.11	0.83	0.92	2.82	0.70	1.19	1.06	0.92	3.67	3.62	2.12	4.76	7.00	7.43
Ho	0.34	0.49	0.21	0.15	0.18	0.57	0.14	0.23	0.22	0.19	0.73	0.71	0.45	0.97	1.45	1.55
Er	0.96	1.38	0.59	0.44	0.51	1.58	0.38	0.75	0.65	0.60	2.14	2.09	1.45	2.92	4.52	4.72
Tm	0.13	0.19	0.08	0.06	0.07	0.21	0.06	0.10	0.11	0.09	0.29	0.29	0.21	0.44	0.72	0.73
Yb	0.85	1.27	0.59	0.41	0.48	1.40	0.38	0.67	0.70	0.69	2.07	2.06	1.60	3.07	5.01	5.11

Table 2 (continued)

Sample	PG-P YD203	PG-P YD-34	PG-P TW208	PG-P TW203	PG-P TW306	PG-P TW18	PG-P RY-1[a]	PG-P RY-2[a]	PG-P TW-33	PG-P TW-35	B TW206-2	B TW202-1	A YD305	A TW201	Q-P YD205-1	Q-P YD205-2
Lu	0.11	0.20	0.08	0.05	0.07	0.21	0.07	0.11	0.12	0.11	0.29	0.29	0.25	0.48	0.75	0.74
ΣREE	40.46	48.68	55.88	36.02	37.68	91.98	24.87	43.48	37.43	46.80	85.09	105.7	61.62	90.07	218.3	227.9
δEu	1.15	1.124	1.37	1.56	1.47	1.01	1.35	1.32	1.23	0.98	1.30	1.19	0.98	1.12	0.23	0.23
Sr/Y	82.6	26.1	100	78.5	133	57.6			50.9	49.3	34.2	43.4	25.3	31.6	1.67	0.82
La/Yb	7.39	5.30	19.3	18.0	16.1	11.8	13.6	13.1	10.5	14.4	6.91	8.16	6.01	4.07	8.10	8.16

Major elements by XRF; trace elements by ICP-MS
$Mg^{\#}=100\times Mg^{2+}/(Mg^{2+}+Fe^{2+})$
PG-P Plagiogranite porphyry, *B* basalt, *A* andesite, and *Q-P* quartz porphyry
[a]Rui et al. 2002

$[(Mg^{\#}=100\times Mg^{2+}/(Mg^{2+}+Fe^{2+})]$ is moderately high ranging from 40–48. The TFeO and CaO contents of the plagiogranite porphyries range from 1.6–4.5 and 0.3–3.5wt %, respectively, and the P_2O_5 contents from 0.06–0.55wt %. In contrast, the andesites are characterized by high contents of TFeO (7.9–9.6wt%) and MgO (3.7–4.0wt%). The postore quartz porphyries show low $Mg^{\#}$ values (31–38) and Al_2O_3 contents (12.1–12.7wt%) and high SiO_2 contents (76.6–78.8wt%).

Figure 5a shows N-type mid-ocean-ridge basalt (MORB)-normalized trace element patterns of the plagiogranite porphyries. These patterns indicate that trace element concentrations have regular variations. Large-ion lithophile elements (LILE) Rb, K, Th, and Sr are highly enriched, while the high-field strength elements (HFSE) Nb, Ta, and Ti and the heavy rare-earth element (HREE) Yb are strongly depleted. The strong depletion of Yb in Fig. 5a is probably related to garnet in the magma source (Sun and Stern 2001). In spite of their lower degrees of LILE-enrichment and HREE depletion, the andesites are generally similar to the ore-bearing plagiogranite porphyries in trace element patterns and enriched and depleted element characteristics (Fig. 5a). In contrast, the postore quartz porphyries show different trace element patterns compared to the plagiogranite porphyries.

The rare-earth elements (REEs) of the plagiogranite porphyries at Tuwu show similar patterns to those at Yandong with a total REE content of 25–92 ppm and notably LREE/HREE fractionation (La/Yb=5.3–19.3). On a chondrite-normalized REE diagram (Fig. 5b), the samples from the Tuwu–Yandong area show positive Eu anomalies (δEu=0.98–1.56). In contrast, the quartz porphyries have marked negative Eu anomalies and high Yb and Y values that are different from those of the plagiogranite porphyries.

Sr-Nd-Pb isotope compositions

The Sr-Nd-Pb isotope compositions of the Tuwu and Yandong copper deposits are listed in Tables 3 and 4 and shown in Figs. 6 and 7. The $\varepsilon_{Nd(t)}$ and initial $^{87}Sr/^{86}Sr$ values of the plagiogranite porphyries are +5.0 to +9.4 and 0.70316 to 0.70378, respectively. Basalts, andesites, ores, and plagiogranite porphyries show similar Sr-Nd isotope compositions (Table 3). The Nd and Sr isotope compositions of the plagiogranite porphyries are close to those of most subduction-related adakites that have MORB-like isotope compositions (Fig. 6). The $^{206}Pb/^{204}Pb$, $^{207}Pb/^{204}Pb$, and $^{208}Pb/^{204}Pb$ values of plagiogranite porphyries are 17.791–18.360, 15.395–15.446, and 37.305–37.672, respectively (Table 4). The data reflect that the Pb isotope ratios are relatively uniform. In the plumbotectonic diagram of Zartman and Doe (1981), the plagiogranite porphyries plot close to the mantle line (Fig. 7). The ores from Tuwu and Yandong have different Pb isotope compositions. The Yandong ores show uniform Pb isotope compositions and mantle-Pb characteristics,

Table 3 Sr and Nd isotope data of Tuwu–Yandong plagiogranite porphyry (PG-P), basalt (B), andesite (A), quartz porphyry (Q-P), and ore (Py + Ccp)

Number	Sample	$Rb\times10^{-6}$	$Sr\times10^{-6}$	$^{87}Rb/^{86}Sr$	$^{87}Sr/^{86}Sr\pm2\sigma$	$(^{87}Sr/^{86}Sr)_i$	ϵ_{Sr}	$Sm\times10^{-6}$	$Nd\times10^{-6}$	$^{147}Sm/^{144}Nd$	$^{143}Nd/^{144}Nd\pm2\sigma$	$(^{143}Nd/^{144}Nd)_i$	ε_{Nd}
R-01[a]	PG-P	20.07	623.8	0.09316	0.703877±12	0.70340	−12			0.1235	0.512944		9.4
R-02[a]	PG-P	19.05	390.6	0.1412	0.704099±11	0.70342	−11			0.1126	0.512806		7.2
R-03[a]	PG-P	25.85	456.9	0.1638	0.703955±14	0.70316	−17			0.1119	0.512812		7.4
R-04[a]	PG-P	20.15	327.2	0.1783	0.704175±13	0.70331	−14			0.1175	0.512870		8.0
R-05[a]	PG-P	74.44	744.0	0.2897	0.704987±14	0.70358	−11			0.1368	0.512421		−1.4
R-06[a]	PG-P	58.04	452.1	0.3717	0.704975±11	0.70318	−18			0.1012	0.512767		7.0
R-07[a]	PG-P	65.08	293.2	0.6427	0.706739±24	0.70363	−13			0.1038	0.512730		6.2
YD203	PG-P	19.89	472.7	0.1234	0.704377±17	0.70378	−4.4	2.509	11.27	0.1347	0.512757±13	0.5124571	5.0
TW208	PG-P	39.75	630.1	0.1816	0.704286±11	0.70341	−9.7	1.771	9.821	0.1092	0.512744±9	0.5125009	5.9
TW203	PG-P	30.89	320.8	0.2773	0.704783±10	0.70344	−9.2	1.115	6.177	0.1093	0.512773±11	0.5125297	6.4
TW204	PG-P	37.67	552.1	0.1967	0.704250±13	0.70330	−11.2	2.433	11.55	0.1275	0.512824±12	0.5125402	6.6
TW219	PG-P	18.99	679.1	0.081	0.703898±13	0.70351	−8.3	4.159	19.89	0.1266	0.512872±11	0.5125902	7.6
TW202-1	B	19.79	879.7	0.0649	0.703793±14	0.70347	−8.6	4.484	21.08	0.1288	0.512826±18	0.5125308	6.7
TW206-1	B	8.112	978.1	0.0238	0.703811±14	0.70369	−5.5	4.294	20.10	0.1298	0.512855±13	0.5125587	7.3
TW206-2	B	3.095	709.2	0.0127	0.704022±18	0.70396	−1.7	4.895	20.95	0.1415	0.512861±13	0.5125367	6.8
TW201	A	4.199	707.2	0.017	0.703713±13	0.70363	−6.4	4.211	16.60	0.1535	0.512859±12	0.5125072	6.2
YD205-1	Q-P	47.48	54.99	2.497	0.714914±13	0.70461	6.5	7.583	37.74	0.1216	0.512779±12	0.5125482	5.5
YD205-2	Q-P	52.50	31.82	2.059	0.713154±12	0.70466	7.2	7.711	38.40	0.1216	0.512769±13	0.5125382	5.3
TWK205	Py + Ccp	1.322	44.57	0.085	0.704030±13	0.70363	−6.7	0.1285	0.7565	0.1028	0.512724±17	0.5125019	5.6
TWK207	Py + Ccp	2.470	48.98	0.1447	0.704246±12	0.70357	−7.6	0.9542	3.978	0.1452	0.512866±17	0.5125523	6.6

Analyzed by isotopic laboratory of Institute of Geology and Geophysics, Chinese Academy of Sciences. The initial $^{87}Sr/^{86}Sr$ and ε_{Nd} values of PG-P, B, A, and ores were calculated at t=330 Ma, except those of Q-P at t=290 Ma. Other parameters for calculation: $(^{143}Nd/^{144}Nd)_{CHUR,0}=0.512638$, $(^{147}Sm/^{144}Nd)_{CHUR,0}=0.1967$, $\lambda^{87}Rb=1.42\times10^{-11}a^{-1}$, and $\lambda^{147}Sm=6.54\times10^{-12}a^{-1}$

Py Pyrite and *Ccp* chalcopyrite

[a]Rui et al. (2004)

Table 4 Pb isotopic composition of plagiogranite porphyry and pyrite

Number	Sample	$^{208}Pb/^{204}Pb$	$^{207}Pb/^{204}Pb$	$^{206}Pb/^{204}Pb$
TW203	Plagiogranite	37.3519	15.4063	17.7912
TW204	porphyry	37.5373	15.4375	17.9285
TW205-1		37.3561	15.4146	17.8031
TW205-3		37.3049	15.3946	17.8292
TW208		37.6719	15.4464	18.3214
YD201-1		37.4207	15.4338	17.8730
YD201-2		37.3439	15.4090	17.8384
YD203		37.3540	15.4296	18.3599
TW305k	Pyrite	38.1774	15.5538	18.2780
TW307k		38.0622	15.5385	18.0403
TW315k		38.4641	15.5982	18.3852
YD301k		37.4782	15.4612	17.8182
YD302k		37.4822	15.4623	17.8188
YD303k		37.4765	15.4623	17.8219

while the Tuwu ores are characterized by significant variations in Pb isotope values.

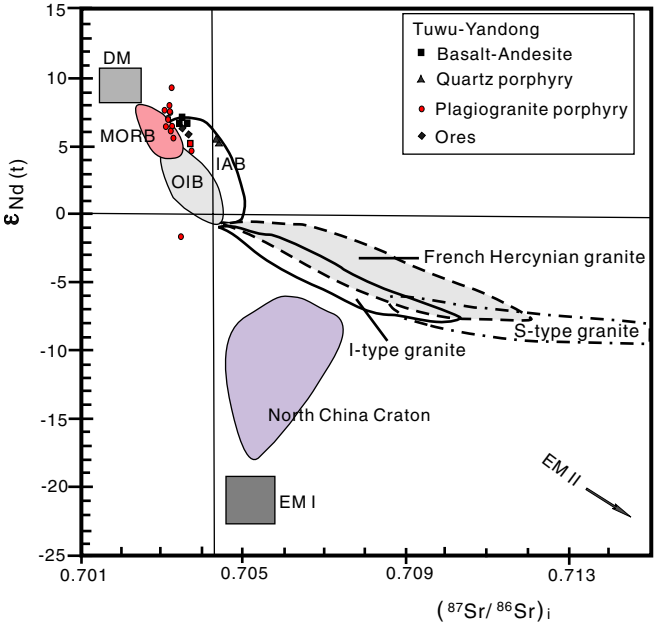

Fig. 6 Diagram of $\varepsilon_{Nd(t)}$ vs $(^{87}Sr/^{86}Sr)_i$ of ores, plagiogranite porphyries, and other rocks in the Tuwu–Yandong copper belt. DM, MORB, IAB, OIB, EMI, and EMII after Zindler and Hart (1986); French Hercynian granites, Australian Paleozoic I- and S-type granites after McCalloch and Chappell (1982); North China craton after Zhang et al. (2001)

Discussion

Adakite affinity of the ore-bearing plagiogranite porphyries

Typical adakites are characterized by ≥56wt% SiO, ≥15wt% Al_2O_3 (rarely lower), usually <3wt% MgO (rarely above 6wt %), low Y and HREE (e.g., Yb <1.9 ppm, Y <18 ppm), high Sr (rarely <400 ppm), low abundance of HFSE, and usually <0.7040 $^{87}Sr/^{86}Sr$ (Defant and Drummond 1990). Except for the postore quartz porphyries and andesites, the bulk of the ore-bearing plagiogranite porphyries in the Tuwu–Yandong copper belt are comparable to the above values. Their Al_2O_3 contents range from 14 to 17wt% with an average of 15.8wt %. High Sr concentrations ranging from 347 to 920 ppm with an average of 563 ppm and low $^{87}Sr/^{86}Sr$ ratios between 0.7032 and 0.7038 are consistent with those of adakites. Yb and Y contents range from 0.4 to 1.4 ppm with an average of 0.7 ppm and 3.4 to 16.0 ppm with an average of 7.6 ppm (Table 2), respectively; these values are much lower than those of other adakites. The above data demonstrate that the ore-bearing plagiogranite porphyries of the Tuwu and Yandong copper belt show a geochemical affinity with adakites.

In the Sr/Y vs Y diagram (Fig. 8), the plagiogranite porphyries plot in the adakite field, indicating a geochemical affinity with ore-bearing porphyries in Chile (Oyarzún et al. 2001) and with the evolution of MORB. In contrast, andesites of the Qiershan Group plot in the field of normal

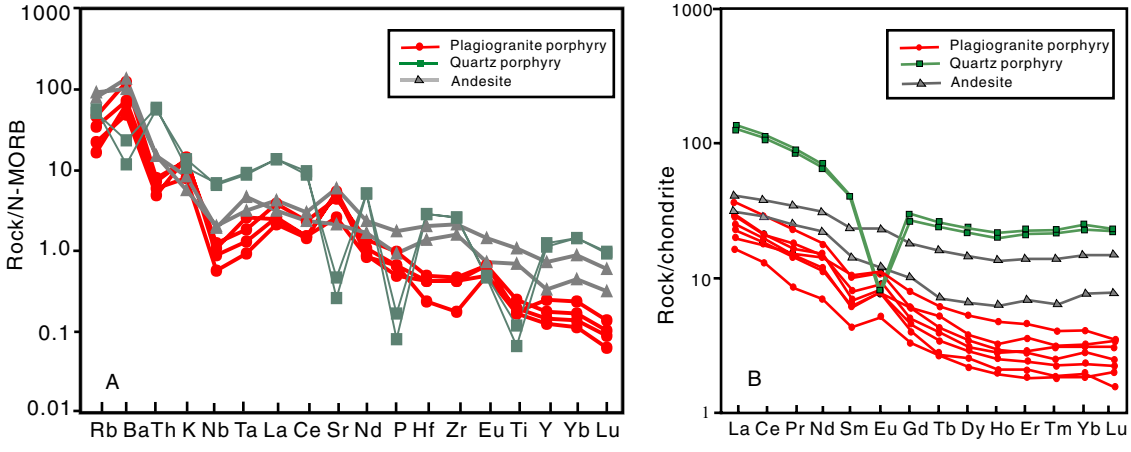

Fig. 5 **a** MORB-normalized trace-element patterns of plagiogranite porphyries (Bevins et al. 1984). **b** Chondrite-normalized REE patterns of plagiogranite porphyries (Boynton 1984)

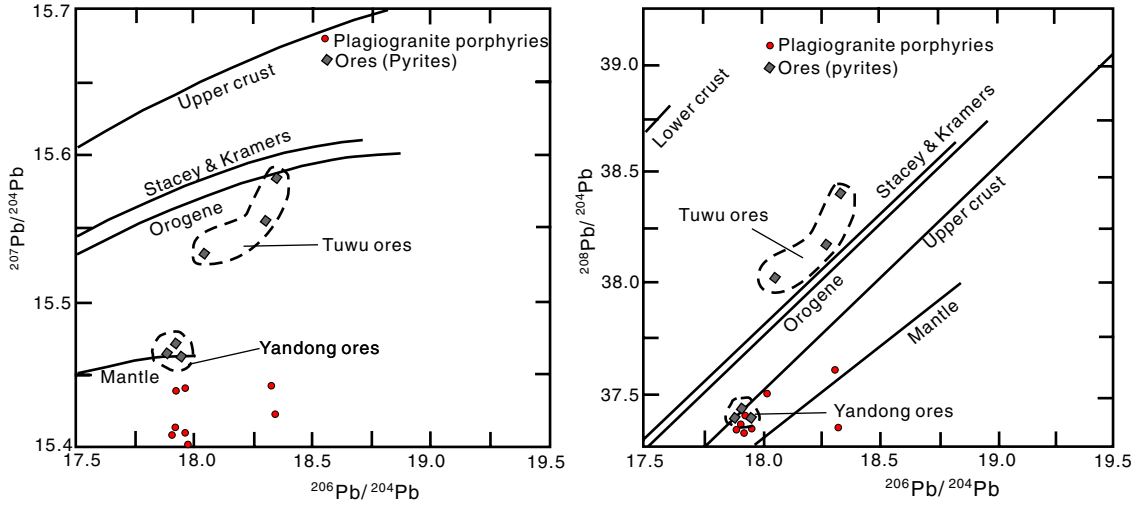

Fig. 7 Pb isotopic geotectonic framework diagrams of the plagiogranite porphyries and ores in the Tuwu–Yandong copper belt (Zartman and Doe 1981)

volcanic arc rocks (Fig. 9). The adakites have remarkably higher Sr/Y (30–140) and La/Yb (5–20) ratios than contemporaneous and barren magmatic rocks (e.g., volcanic rocks of the Qiershan Group and quartz porphyry) in the same island arc belt (Table 2).

In spite of the fact that the adakites and arc volcanic rocks of the Tuwu–Yandong ore belt show some differences in geochemistry (e.g., the former are lower in Y and Yb concentrations), they have the same signatures as arc volcanic rocks such as clear depletion of Nb and other HFSE and enrichment of LILE (Fig. 6a). These relations demonstrate that the early Carboniferous volcanic rocks and adakites in the Dananhu area formed in the same island arc setting, although they are different in their formation mechanism and magma origin.

Based on geochemical characteristics, such as those of Nd and Sr isotopes close to those of MORB (Fig. 7), high $Mg^{\#}$ (>40) values, low Y concentrations, and a distribution along the partial melting line in the La/Sm vs La diagram (Fig. 9), we infer that the adakites in the Tuwu–Yandong copper belt were most likely derived by partial melting of a subducting oceanic slab. Based on the formation conditions of adakites (Sen and Dunn 1994; Martin 1999; Rapp et al. 1999; Defant et al. 2002), we further suggest that the ore-bearing plagiogranite porphyries formed during fast and oblique convergence between the paleo-Tianshan ocean and the Dananhu arc, which yielded magmas of adakitic affinity (Defant and Drummond 1990; Oyarzún et al. 2001). Under compressional conditions, the absence of volcanism prevents the escape of SO_2 from sulfur-rich and highly oxidized adakitic magmas (closed porphyry system) facilitating the formation of huge copper deposits (Oyarzún et al. 2001).

Based on the fact that volcanic rocks, consisting of basalt, andesite, and dacite in the Dananhu district, are characteristic of normal arcs and have calc-alkaline geochemistry, we infer that these rocks formed by partial melting of the mantle wedge and underwent crystal fractionation before the plagiogranite porphyries were intruded.

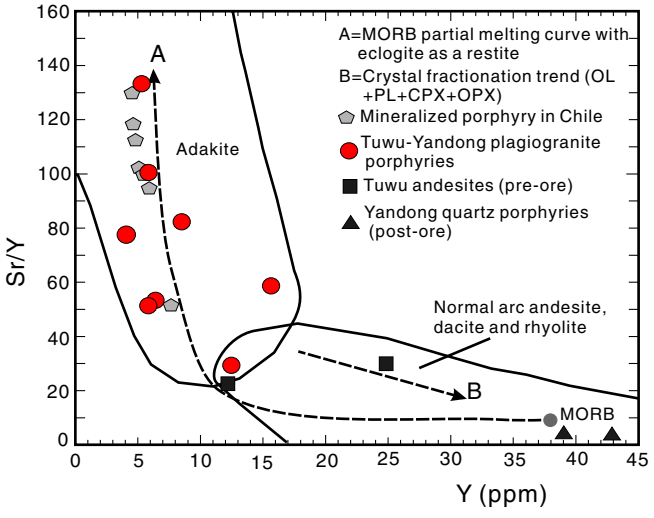

Fig. 8 Diagram of Sr/Y vs Y (Defant and Drummond 1993). The data on mineralized porphyries in Chile are from Oyarzún et al. (2001)

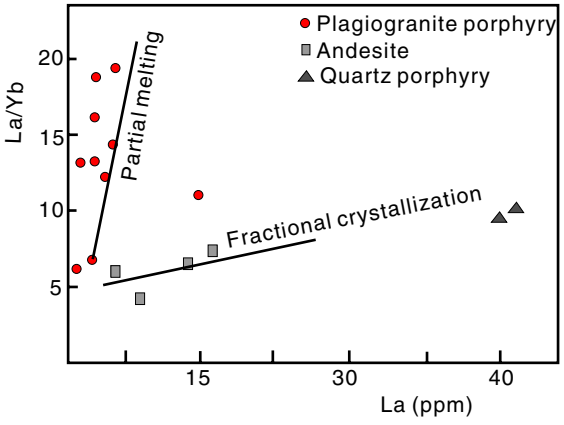

Fig. 9 Diagram of La/Yb vs La for the plagiogranite porphyries and volcanic rocks

Favorable ore-forming conditions of adakite

There was growing interest in adakitic magmatism and its relation to copper and gold mineralization in the last decade. In the Chilean Andes where world-class copper deposits are clustered, adakitic rocks are associated with Oligocene porphyry copper deposits, suggesting a metallogenic connection between such magmatism and porphyry copper mineralization (Thiéblemont et al. 1997). Adakites are associated with gold and copper mineralization in the Philippines (Sajona and Maury 1998). Oyarzún et al. (2001) suggested that huge porphyry copper deposits (e.g., Chuquicamata) are related to adakitic rocks, whereas small porphyry copper deposits have normal calc-alkaline affinity. Zhang et al. (2001, 2002) proposed that porphyry copper deposits worldwide are mostly related to adakites. They proposed that giant porphyry copper deposits are related to adakitic, highly oxidized, and water-rich melts and also suggested that these melts were eventually derived from slab melting during flat subduction.

Based on studies of experimental petrology and metallogeny (Drummond and Defant 1990; Hendenquist 1994; Sen and Dunn 1994; Kay and Mpodozis 2001; Defant et al. 2002; Mungall 2002; Wang et al. 2003), it is widely accepted that MORB (basaltic oceanic crust) characterized by high abundance of Cu, Au, and volatile components such as H_2O and Cl is the dominant source of adakitic rocks. During the generation of adakites, large-scale decomposition of amphibole within subducted oceanic crust releases large amounts of H_2O, Cl, Cu, and Au into the adakitic magmas. As a result of rapid pressure decrease during ascent, the magmas release Cu, Au, and volatiles leading to the formation of ore-forming fluids. During the entire process from magma generation through magma ascent and interaction with the mantle wedge to the final stage of fluid release from the magma, high oxygen fugacity (fO_2) is necessary, which will restrain the stability of sulfides and allow Cu and Au enrichment in the magma.

Analyses show that biotite in the plagiogranite porphyries is magnesium-rich with Mg/(Mg+Fe+Mn) values of 0.35–0.60 (Rui et al. 2002) and significant amounts of hematite and magnetite are observed in polished sections of the ores. We infer that the plagiogranite porphyries formed at high oxygen fugacity (fO_2). On the other hand, microfissures were developed at the porphyry tops and in their wallrocks. The porphyries are cut by numerous quartz-sulfide and chlorite-sulfide veinlets and locally by carbonate veinlets with minor sulfides.

As reported by Han et al. (2003), the $\delta^{34}S$ composition of sulfides in the Tuwu and Yandong deposits ranges from −0.9 to +1.3‰ and is very close to that of mantle sulfur, indicating a deep sulfur source. In fact, sulfur isotopes in global porphyry copper deposits genetically related to subducted oceanic crust cluster near 0‰ (Han et al. 2003). The measured $\delta^{18}O$ values are 7.0 to 9.7‰ for quartz and chlorite, respectively. The δD values of fluid inclusions in quartz, chlorite, and sericite fall into the range of −44 to −66‰ (Rui et al. 2002), indicating that magmatic water was involved in the ore-forming process.

Significance of the Tuwu–Yandong adakites

A variety of models for adakite generation was proposed, such as partial melting of an oceanic slab related to incipient or flat subduction (Defant and Drummond 1990, 1993; Gutscher et al. 2000; Oyarzún et al. 2001; Reich et al. 2003), partial melting of basaltic lower crust (Stern and Killian 1996; Kay and Mpodozis 2001; Chung et al. 2003), assimilation and fractional crystallization processes (Castillo 2002), and partial melting of slab window margins (Thorkelson and Breitsprecher 2004). Based on geologic and geochemical data, we would suggest that the porphyry copper deposits of the Tuwu–Yandong copper belt formed in a volcanic island arc setting and that adakite magmatism was induced by flat subduction of the oceanic slab. In contrast, the volcanic rocks were formed in a normal island arc setting during the early Carboniferous.

In the Dananhu area, the Devonian-Carboniferous volcanic arc contains a forearc-backarc-accretionary wedge and was generated by northward subduction of the paleo-Tianshan ocean (Li et al. 2002; Zhang et al. 2004a; Xiao et al. 2004; Mao et al. 2004). Because adakites are related to oceanic plate subduction, the distribution of the adakites in the belt peripheral to the Tupan–Hami (Tuha) basin further indicates that the Tianshan oceanic crust subducted northwards beneath the Paleozoic Dananhu arc in the late Devonian-early Carboniferous. The main formation condition of the Paleozoic adakites is rapid subduction of a low- or flat-angle oceanic slab.

The plagiogranite porphyries are spatially and temporally associated with copper mineralization. This is shown by the fact that mineralization ages are close to those of the plagiogranite porphyries, and the main copper ore bodies are hosted and accompanied by hydrothermal alteration of the porphyries. Therefore, we suggest that the occurrence of adakite can be taken as potential prospecting targets. One such target in China is the late Paleozoic Central Asian orogen.

Conclusions

The Tuwu–Yandong copper belt is the largest porphyry copper belt in NW China. Based on detailed study of the ore-bearing plagiogranite porphyries in two copper deposits (Tuwu and Yandong), we arrive at the following main conclusions:

(a) The ore-bearing porphyries of the Tuwu–Yandong copper belt have intrusive ages of 360–330 Ma and were formed as a result of early Carboniferous subduction. Petrochemically, they belong to the calc-alkaline series with enrichment in LILE Rb, K, Th, and Sr and depletion in the HSFE Nb, Ta, and Ti, and the HREE Yb, indicating the important role of subduction-related components in the process of magma generation.
(b) The ore-bearing porphyries possess the diagnostic characteristics of adakites including ≥56wt% SiO, ≥5wt% Al_2O_3, <3wt% MgO, low Y content (3.4–

16.0 ppm), low Yb content (0.4–1.4 ppm), high Sr (346–920 ppm), and positive Eu anomalies. These rocks also show positive $\varepsilon_{Nd(t)}$ values (+5.0–+9.4) and low initial $^{87}Sr/^{86}Sr$ values of 0.7032–0.7038. The Nd and Sr isotope compositions are similar or close to those of most subduction-related adakites. All these characteristics suggest that the ore-bearing porphyries were the result of partial melting of a subducted oceanic slab $\varepsilon_{Nd(t)}$.

(c) The copper porphyry systems in the Tuwu and Yandong ore belt have relatively high oxygen fugacity (fO_2). Plagiogranite porphyry is spatially and temporally associated with copper mineralization and thus can be considered as a new exploration target applicable to the search for porphyry copper deposits.

Acknowledgements This research was financially supported by National Natural Science Foundation (NSFC grant 40473028), Major State Basic Research Program of People's Republic of China (No. 2001CB409805), and CAS Knowledge Innovation Project (KZCX3-SW-137). Thanks are given to JW Mao, WQ Li, and CM Han for thoughtful discussions and for providing relevant references. The authors appreciate BF Windley and LX Gu for their improvement of the English.

References

Allen MB, Windley BF, Zhang C (1992) Palaeozoic collisional tectonic and magmatism of the Chinese Tianshan, central Asia. Tectonophysics 220:89–115

Bevins RE, Kokelar BP, Dunkley PN (1984) Petrology and geochemistry of lower to middle Ordovician igneous rocks in Wales: a volcanic arc to marginal basin transition. Proc Geol Assoc 95:337–347

Boynton WV (1984) Geochemistry of the rare earth elements: meteorite studies. In: Henderson P (ed) Rare earth elements geochemistry. Elsevier, Amsterdam, pp 63–114

Castillo PR (2002) The origin of some of the adakite-like and Nb-enriched lavas in southern Philippines. Acta Petrol Sin 18:143–151

Chen F, Satir M, Ji J, Zhong D (2002) Nd-Sr-Pb isotopic composition of the Cenozoic volcanic rocks from western Yunnan, China: evidence for enriched mantle source. J Asian Earth Sci 21:39–45

Chung SL, Liu DY, Ji JQ, Chu MF, Lee HY, Wen DJ, Lo CH, Lee TY, Qian Q, Zhang Q (2003) Adakites from continental collision zones: melting of thickened lower crust beneath southern Tibet. Geology 31:1021–1024

Defant MJ, Drummond MS (1990) Derivation of some modern arc magmas by melting of young subduction lithosphere. Nature 347:662–665

Defant MJ, Drummond MS (1993) Mount St. Helens: potential example of the partial melting of the subducted lithosphere in a volcanic arc. Geology 21:547–550

Defant MJ, Xu JF, Kepezhinskas P, Wang Q, Zhang Q, Xiao L (2002) Adakites: some variations on a theme. Acta Petrol Sin 18:129–142

Drummond MS, Defant MJ (1990) A model for trondhjemite-tonalite-dacite genesis and crustal growth via slab melting: Archean to modern comparison. J Geophys Res 95:21503–21521

Gu LX, Hu SX, Chu Q, Yu CS, Xiao XJ (1999) Pre-collision granites and post-collision intrusive assemblage of the Kelameili–Harlik orogenic belt. Acta Geol Sin (English edition) 73:316–329

Gu LX, Hu SX, Yu CS, Wu CZ, Yan ZF (2001) Initiation and evolution of the Bogda subduction-torn-type rift (in Chinese with English abstract). Acta Petrol Sin 17:585–597

Gutscher MA, Maury R, Eissen JP, Bourdon E (2000) Can slab melting be caused by flat subduction. Geology 28:535–538

Han CM, Rui Z, Mao JW, Yang JM, Wang ZL (2003) Geological characteristics of the Tuwu copper deposit, Hami, Xinjiang. In: Mao JW, Goldfarb RJ, Seltmann R, Wang, DH, Xiao WJ, Hart C (eds) Tectonic evolution and metallogeny of the Chinese Altay and Tianshan. Proceedings volume of the international symposium of the IGCP-473 project in Urumqi, pp 249–260

He GQ, Li MS, Liu DQ (1994) Palaeozoic crustal evolution and mineralisation in Xinjiang of China (in Chinese with English abstract). Xinjiang People's Publishing House, Urimqi, pp 62–245

Hendenquist JW (1994) The role of magmas in the formation of hydrothermal ore deposits. Nature 370:519–527

Hou ZQ, Gao YF, Qu XM, Rui ZY, Mo XX (2004) Origin of adakitic intrusives generated during mid-Miocene east–west extension in southern Tibet. Earth Planet Sci Lett 220:139–155

Kay SM, Mpodozis C (2001) Central Andean ore deposits linked to evolving shallow subduction systems and thickening crust. GSA Today 11:4–9

Li JY, Wang KZ, Li WQ, Guo HC, Song B, Wang Y (2002) Tectonic evolution since the late Paleozoic and mineral prospecting in eastern Tianshan Mountains, NW China (in Chinese with English abstract). Xinjiang Geology 20:295–301

Liu DQ, Chen YC, Wang DH (2003) A discussion on problems related to mineralisation of Tuwu–Yandong Cu-Mo Ore field in Hami, Xinjiang (in Chinese with English abstract). Miner Depos 22:334–344

Ma RS, Shu LS, Sun JQ (1997) Tectonic evolution and metallogeny of eastern Tianshan mountains (in Chinese with English abstract). Geological Publishing House, Beijing, p 202

Martin H (1999) Adakitic magmas: modern analogues of archaean granitoids. Lithos 46:411–429

Mao JW, Goldfarb RJ, Wang YT, Hart CJ, Wang ZL, Yang JM (2004) Late Paleozoic base and precious metal deposits, East Tianshan, Xinjiang, China: characteristics and geodynamic setting. Episodes 28:1–14

McCalloch MT, Chappell BW (1982) Nd isotopic characteristics of S- and I-type granites. Earth Planet Sci Lett 58:51–64

Mungall JE (2002) Roasting the mantle: slab melting and the genesis of major Au and Au-rich Cu deposits. Geology 30:915–918

Oyarzún R, Márquez A, Lillo J, López I, Rivera S (2001) Giant versus small porphyry copper deposits of Cenozoic age in northern Chile: adakitic versus normal calc-alkaline magmatism. Miner Depos 36:794–798

Perello J, Cox D, Garamjav D (2001) Oyu Tolgoi, Mongolia; Siluro-Devonian porphyry Cu-Au-(Mo) and high-sulfidation Cu mineralisation with a Cretaceous chalcocite blanket. Econ Geol 96:1407–1428

Qin KZ, Sun S, Fang TH, Wang SL, Liu W (2002) Paleozoic epithermal Au and porphyry Cu deposits in North Xinjiang, China: epochs, features, tectonic linkage and exploration significance. Resour Geol 52:291–300

Qin KZ, Zhang LC, Xiao WJ, Xu XW, Yan Z, Mao JW (2003) Overview of major Au, Cu, Ni and Fe deposits and metallogenic evolution of the eastern Tianshan mountains, Northwestern China. In: Mao JW, Goldfarb RJ, Seltmann R, Wang, DH, Xiao WJ, Hart C (eds) Tectonic evolution and metallogeny of the Chinese Altay and Tianshan. Proceedings volume of the international symposium of the IGCP-473 project in Urumqi, pp 227–248

Qu XM, Hou ZQ, Li YG (2004) Melt components derived from a subducted slab in late orogenic ore-bearing porphyries in the Gangdese copper belt, southern Tibetan plateau. Lithos 74:131–148

Rapp RP, Shimizu N, Norman MD (1999) Reaction between slab-derived melts and peridotite in the mantle wedge: experimental constraints at 3.8 GPa. Chem Geol 160:335–356

Reich M, Parada MA, Palacios C, Dietrich A, Schultz F, Lehmann B (2003) Adakite-like signature of Late Miocene intrusions at the Los Pelambres giant porphyry copper deposit in the Andes of central Chile: metallogenic implications. Miner Depos 38:876–885

Rui ZY, Wang LS, Wang YT, Liu YL (2002) Discussion on metallogenic epoch of Tuwu and Yandong porphyry copper deposits in East Tianshan Mountains, Xinjiang (in Chinese with English abstract). Miner Depos 21(1):16–22

Rui ZY, Zhang LS, Chen ZY, Wang LS, Liu YL, Wang YT (2004) Approach on source rock or source region of porphyry copper deposit (in Chinese with English abstract). Acta Petrol Sin 20:229–238

Sajona FG, Maury RC (1998) Association of adakites with gold and copper mineralisation in Philippines. C R Acad Sci Paris Earth Planet Sci 326:27–34

Sen C, Dunn T (1994) Dehydration melting of a basaltic composition amphibolite at 1.5 and 2.0 GPa: implications for the origin of adakites. Contrib Mineral Petrol 117:394–409

Stern CR, Killian R (1996) Role of the subducted slab, mantle wedge and continental crust in the generation of adakites from the Andean Austral Volcanic Zone. Contrib Mineral Petrol 123:263–281

Sun CH, Stern RJ (2001) Genesis of Mariana shoshonites: contribution of the subduction component. J Geophys Res 106(B1):589–608

Thiéblemont D, Stein G, Lescuyer JL (1997) Gisements épithermaux et porphyriques: la connexion adakite. Earth Planet Sci 325:103–109

Thorkelson DJ, Breitsprecher K (2004) Partial melting of slab window margins: genesis of adakitic and on-adakitic magmas. Lithos 79:25–41

Xiao WJ, Zhang LC, Qin KZ, Sun S, Li JL (2004) Paleozoic accretionary and collisional tectonics of the Eastern Tianshan (China): implications for the continental growth of central Asia. Am J Sci 304:370–395

Xiong XL, Zhao ZH, Bai ZH, Mei HJ, Xu JF, Wang Q (2001) Origin of Awulale adakitic sodium-rich rocks in western Tianshan: constraints for Nd and Sr isotopic compositions (in Chinese with English abstract). Acta Petrol Sin 17:514–522

Xu JF, Mei HJ, Yu XY (2001) Adakites related to subduction in the northern margin of Junggar arc for the late-Paleozoic: products of slab melting. Chin Sci Bull 46:68–688

Wang FT, Feng J, Hu JW (2001) The characteristics and significance of Tuwu large-type porphyry copper deposit in Xinjiang (in Chinese with English abstract). Chin Geol 28:36–39

Wang Q, Xu JF, Zhao ZH (2003) Intermediate-acid igneous rocks strongly depleted in heavy rare earth elements (or adakitic rocks) and copper–gold metallogenesis (in Chinese with English abstract). Earth Science Frontiers 10:561–572

Windley BF, Allen MB, Zhang C (1990) Palaeozoic accretion and Cenozoic redeformation of the Chinese Tianshan range, Central Asia. Geology 18:128–131

Zartman RE, Doe BR (1981) Plumbotectonics—the model. Tectonophysics 75:135–162

Zhang Q, Wang Y, Qian Q (2001) The characteristics and tectonic-metallogenic significance of the Mesozoic adakites in eastern China (in Chinese with English abstract). Acta Petrol Sin 17:236–244

Zhang Q, Wang Y, Liu W, Wang YL (2002) Adakite: Its characteristics and implications (in Chinese with English abstract). Geol Bull China 2:431–435

Zhang LC, Shen YC, Ji JS (2003) Characteristics and genesis of Kanggur gold deposit in the eastern Tianshan mountains, NW China: evidence from geology, isotope distribution and chronology. Ore Geol Rev 23:71–90

Zhang LC, Xiao WJ, Qin KZ, Ji JS, Yang XK (2004a) Types, geological features and geodynamic significance of gold–copper deposits in the Kanggurtag metallogenic belt, eastern Tianshan, NW China. Int J Earth Sci 93:224–240

Zhang LC, Qin KZ, Yang JF, Xia B, Shu JS (2004b) The relationship between ore-forming processes and adakitic rock in Tuwu–Yandong porphyry copper metallogenic belt, eastern Tianshan mountains (in Chinese with English abstract). Acta Petrol Sin 20:259–268

Zhang LC, Xiao WJ, Qin KZ, Qu W J, Du AD (2005) Re-Os isotopic dating of molybdenite and pyrite in the Baishan Mo-Re deposit, eastern Tianshan, NW China, and its geological significance. Miner Depos 39:960–969

Zindler A, Hart SR (1986) Chemical geodynamics. Ann Rev Earth Plant Sci 14:493–571